Reorientation dynamics of nanoconfined water: Power-law decay, hydrogen-bond jumps, and test of a two-state model

Damien Laage[1,a)] and Ward H. Thompson[2,b)]
[1]*Department of Chemistry, Ecole Normale Supérieure, UMR ENS-CNRS-UPMC 8640, 24 rue Lhomond, 75005 Paris, France*
[2]*Department of Chemistry, University of Kansas, Lawrence, Kansas 66045, USA*

(Received 3 November 2011; accepted 6 January 2012; published online 25 January 2012)

The reorientation dynamics of water confined within nanoscale, hydrophilic silica pores are investigated using molecular dynamics simulations. The effect of surface hydrogen-bonding and electrostatic interactions are examined by comparing with both a silica pore with no charges (representing hydrophobic confinement) and bulk water. The OH reorientation in water is found to slow significantly in hydrophilic confinement compared to bulk water, and is well-described by a power-law decay extending beyond one nanosecond. In contrast, the dynamics of water in the hydrophobic pore are more modestly affected. A two-state model, commonly used to interpret confined liquid properties, is tested by analysis of the position-dependence of the water dynamics. While the two-state model provides a good fit of the orientational decay, our molecular-level analysis evidences that it relies on an over-simplified picture of water dynamics. In contrast with the two-state model assumptions, the interface dynamics is markedly heterogeneous, especially in the hydrophilic pore and there is no single interfacial state with a common dynamics. © *2012 American Institute of Physics*. [doi:10.1063/1.3679404]

I. INTRODUCTION

Understanding the behavior of water confined on nanometer length scales is of great importance for a broad range of fields, from chemistry to biology to engineering, and covering situations as varied as ion channels,[1] reverse micelles,[2,3] fuel-cell membranes,[4] and carbon nanotubes.[5] Among the different confining environments, silica nanopores have received significant attention, motivated by both their fundamental properties and their relevance to practical applications such as separations, sensing, and catalysis. For example, confinement in silica pores has been observed to lower the crystallization temperature of water (and other liquids), allowing the study of supercooled water at temperatures inaccessible in the bulk.[6] In addition, solvation dynamics measured by time-dependent fluorescence measurements can be considerably slowed upon nanoconfinement of the solvent, sometimes by orders-of-magnitude;[3,7] the motions probed in these experiments are closely related to the reaction coordinates for charge transfer processes, so these results are indicative of the significant effects of confinement on chemistry.

A critical issue is to understand how and how much the properties of water are affected by confinement in silica pores.[8–13] X-ray, neutron diffraction, and nuclear magnetic resonance experiments[14–18] have clearly established that the structure of the interfacial water layer is strongly perturbed. However, the impact of confinement on the water dynamics is comparatively less well understood. Recent studies via optical Kerr effect (OKE) spectroscopy,[8,9] dielectric relaxation,[19] and numerical simulation[20,21] have all observed a slowdown in dynamics upon confinement, more pronounced for hydrophilic pores than for hydrophobic ones. However, a molecular picture to understand the origin of this slowdown and thus how surface functionality could be used to tailor water dynamics is still missing.

In this paper, we use molecular dynamics simulations to examine the dynamics of water confined within amorphous silica pores ∼2.4 nm in diameter, focusing on the reorientation and hydrogen(H)-bond dynamics. To investigate the role of surface polarity, we simulate both a hydrophilic, OH-terminated pore and the same pore with all the atom charges set to zero, making it effectively hydrophobic, and compare the results to bulk water. We critically assess whether the popular core/shell, or two-state, description[22,23] which is frequently used in interpreting the results of experimental measurements,[2,3,7] can be justified by a molecular picture. Finally, we provide a molecular interpretation of the key factors governing the interfacial water dynamics by examining the OH-bond reorientation in the context of the recently developed extended jump model for water.[24–26]

II. COMPUTATIONAL METHODOLOGY

Classical molecular dynamics simulations were carried out using the DL_POLY_2 software.[27] Bulk water was simulated using 343 molecules in a cubic box of side-length 21.725311 Å (ρ = 1.00 g/cm^3). The simulations of water confined in silica pores used a rectangular periodic box with dimensions of 30 Å along the pore axis and 44 Å in the perpendicular directions. The number of water molecules was determined by grand canonical Monte Carlo simulations using the Towhee program[28] with a chemical potential of

a)Electronic mail: damien.laage@ens.fr.
b)Electronic mail: wthompson@ku.edu.

−30 kJ/mol, a value that gives a fully water-filled pore. This gave 441 molecules for the normal, hydrophilic silica pore and 416 for the hydrophobic pore with the charges set to zero.

The SPC/E model[29] was used to describe the water interactions. The parameters for the silica force field have been given previously.[30] Lennard-Jones interactions were evaluated with a cutoff of 10.5 Å (15 Å) for bulk (confined) water. Long-range electrostatic interactions were included using three-dimensional periodic boundary conditions with an Ewald summation using $\alpha = 0.25$, a $10 \times 10 \times 10$ k-point grid and a cuttoff of 10.5 Å for bulk water; $\alpha = 0.25$, a $10 \times 10 \times 8$ k-point grid and a cuttoff of 15 Å were used for water in the silica pores.

The bulk water simulation was initiated from a simple cubic lattice and equilibrated for 0.5 ns before a data collection stage of 2 ns. Water confined in the two silica pores was equilibrated for 1 ns before an 8 ns data collection stage during which the configurations were saved every 8 fs. For the hydrophilic pore, the trajectory was extended for an additional 52 ns with configurations saved every 1 ps. In all cases, a 1 fs time step was used. A Nosé-Hoover thermostat[31,32] with a time constant of 1 ps was used to maintain the temperature at 298 K. Error bars were calculated using block-averaging with 10 blocks and reported at a 95% confidence level using the Student t distribution.[33]

III. REORIENTATION DYNAMICS

We follow the reorientation dynamics of the water OH bonds through the time-correlation function

$$C_2(t) = \langle P_2[\mathbf{e}(0) \cdot \mathbf{e}(t)] \rangle, \quad (1)$$

where P_2 is the second Legendre polynomial and, for measurements on water, $\mathbf{e}$ is the unit vector along the OH bond. $C_2(t)$ is a good approximation to the anisotropy decay measured in time-resolved infrared pump-probe experiments.[2,34]

These reorientational correlation functions are plotted in Fig. 1 for water in the bulk as well as in the hydrophilic and hydrophobic pores. These results show that both confinement and the nature of the confining interface have a dramatic impact on the water dynamics.

In bulk water, beyond the initial inertial and librational reorientation (<1 ps), the decay is mono-exponential with a 2.6 ps time scale (63% amplitude). In the hydrophobic pore this bulk time scale persists but its amplitude is reduced (44%) and the difference is taken up by the appearance of at least two additional slower time scales, with characteristic times of 6.3 ps (17%) and >40 ps (0.4%).

In contrast, within the hydrophilic silica pore water reorientation is significantly slower. While the initial decay follows the bulk time scale, at long delays (>20 ps) the correlation function cannot be fit by a sum of exponentials. While, as found previously for silica slit pores,[35] a stretched exponential can satisfactorily fit the short-time decay up to 10 ps, the long-time decay up to delays of 1 ns is best described by a power-law decay, $C_2(t) \propto t^{-1.1}$. Recently, Milischuk and Ladanyi[21] reported the results of simulations of water structure and dynamics in silica pores constructed using the same approach as in the present work. The reorientational

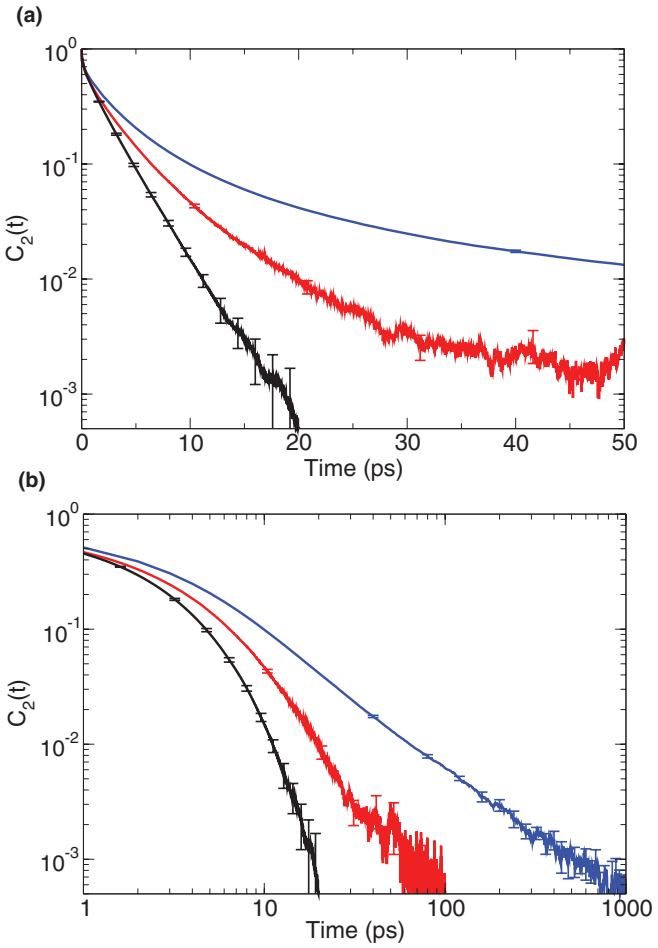

FIG. 1. Water reorientation time correlation function $C_2(t)$, Eq. (1), in hydrophilic (blue) and hydrophobic (red) silica nanopores, together with the bulk reference (black), in log-linear (a) and log-log (b) representations.

dynamics they observed for shorter times, $t < 30$ ps, were also non-exponential, though not characterized as stretched-exponential or power-law. It should be noted that the surface roughness in the amorphous silica pores may also affect the nature of the non-exponential dynamics compared to that for silica slit pores involving comparatively flat interfaces.

Similar power-law behavior was previously observed in OKE measurements on water confined in hydrophilic and hydrophobic (alkyl-terminated) silica pores,[8,9] where the exponent was found to depend sensitively on the pore diameter and on its surface polarity. In particular, in 2.5 nm diameter sol-gel pores it was found that the OKE signal decayed as a power law of the form $t^{-0.33}$ and $t^{-0.07}$ for the hydrophilic and hydrophobic surface chemistries, respectively. For larger pores, ~6 and 10 nm in diameter, the exponent was found to increase in magnitude and a second power law component was required to fit the decay at shorter times. We note that the comparison of the present results with these experiments can only be qualitative for two reasons. First, OKE probes the collective water reorientation, while our calculated $C_2(t)$ follows the single-molecule dynamics. For example, in the bulk liquid, OKE also finds a power-law decay,[8,9] while our simulations yield a single-exponential $C_2(t)$ decay, in quantitative agreement with ultrafast infrared anisotropy experiments.[36] Second, the hydrophobic sol-gel pores used in the OKE

measurements are obtained by functionalizing the surface with alkyl (effectively *tert*-butyl) groups. This both reduces the pore size relative to the hydrophilic case and introduces potential roughness if sufficient space exists between the alkyl groups for water to penetrate to the un-functionalized silica surface.

The presence of such a power-law decay in the reorientational correlation function could be ascribed to a broad (power-law) distribution of reorientation times. Power-law distributions of water relaxation times have been suggested in different confining environments, including MCM-41 nanopores[20] and at the interface with several globular proteins;[37] power-law decays have also been observed for solvation dynamics near DNA.[38–40] Interestingly, the reorientational correlation function has been found to decay as a stretched exponential in simulations of other confined water systems including reverse micelles[41] and silica slit pores.[35] Before investigating the molecular origin of these distributions in nanopores, we first examine whether our results can be described through the popular two-state (or core/shell) model.

IV. TEST OF A TWO-STATE MODEL

The two-state core/shell model has been widely used to interpret the dynamics of confined liquids,[2,3,7] and we now investigate whether its underlying assumptions are supported by our molecular analysis. In this model, it is assumed that only the liquid molecules near the interface with the confining framework (shell) have their properties substantially altered while the pore interior (core) remains bulk-like. It has been shown to provide a good fit of the measured anisotropy decays for water in reverse micelles of diameter >4 nm; for smaller diameters, the core is no longer bulk-like and its contribution progressively disappears with decreasing size.[42] A similar behavior was observed in simulations of water confined in slit pores.[35]

In the context of water OH orientational dynamics, the core/shell model assumes that molecules in the interfacial layer – within a distance Δ of the pore surface – have a modified correlation function, $C_2^{\text{shell}}(t)$, while molecules in the pore interior reorient according to $C_2^{\text{core}}(t)$. The molecular-level implication is a position-dependent correlation function with a sharp transition at the core/shell boundary:

$$C_2(t;d) = C_2^{\text{core}}(t) + \theta(d-\Delta)\left[C_2^{\text{core}}(t) - C_2^{\text{shell}}(t)\right], \tag{2}$$

where d is the distance from the pore wall and $\theta(x)$ is the Heaviside step function. Then, for a cylindrical pore of radius R the overall orientational correlation function is a linear combination of these core and shell results:[22,23,30]

$$C_2^R(t) = C_2^{\text{core}}(t) + \left[C_2^{\text{shell}}(t) - C_2^{\text{core}}(t)\right]\left\{\frac{2\Delta}{R} - \frac{\Delta^2}{R^2}\right\}. \tag{3}$$

Since Δ is typically on the order of the thickness of a molecular layer, the Δ^2/R^2 term is often neglected. Such two-state models have been applied to numerous properties of confined liquids including reorientational dynamics, vibrational and optical spectra, conformational equilibria, and vibrational energy relaxation.[2,3,7] However, a few recent studies have also questioned the adequacy of a two-state description.[30,41,43,44] Often, the two-state model is tested by comparing the observed R-dependence of a given property to the prediction of the model, Eq. (3). In this work, an alternative approach is adopted for two reasons: (1) a single pore size was simulated and (2) the $1/R$ dependence predicted by the two-state model arises from the cylindrical geometry and may not be sufficient to differentiate between different microscopic models. Thus, our main focus lies instead in the molecular-level assumptions in the two-state model, specifically, the d-dependence of $C_2(t; d)$. We therefore examine the range over which the pore wall affects the water dynamics and contrast the situations in the hydrophobic and hydrophilic pores.

Reorientational correlation functions for different initial H positions in the pore, measured by their distance d to the nearest pore oxygen atom, are shown in Fig. 2. In the hydrophilic pore, two main motifs are found for these position-dependent correlation functions. For the water hydrogens closest to the pore surface (d = 2–3 Å), the reorientation follows a power-law which is similar to the average reorientation found for all waters within the pore. At larger distances from the pore wall ($d \geq 5$ Å), the dynamics is nearly bulk-like, with a long time scale that decreases monotonically from 3.5 ps at $d = 5$ Å to 2.8 ps at $d = 8$ Å, compared to 2.6 ps for bulk water. The water structure revealed by the distribution of water positions relative to the pore wall (Fig. 2(c)) shows that these two motifs correspond, respectively, to water molecules initially lying in the interfacial layer and further in the pore center. The intermediate pattern observed for $d = 4$ Å, where the decay is mostly bulk-like with an additional slow component, comes from the partitioning of waters initially between the first and second layers in these two environments with distinct dynamics. This analysis clearly shows that the impact of the pore is mostly limited to the interfacial layer, and that the long-time non-exponential decay of the global $C_2(t)$ arises from these interfacial waters.

In the hydrophobic pore, the position dependence of $C_2(t; d)$ (Fig. 2(b)) is similar to that for the hydrophilic pore, showing that the pore mainly retards the interfacial layer. However, there is a key exception for initial locations closest to the interface (d = 2 Å), where the initial decay of the correlation function is faster than in the bulk. This results from the lack of hydrogen-bonding (H-bonding) partners for these OH bonds at the hydrophobic interface[46,47] which leads to a large inertial component of 49%, nearly three times that for bulk water.

The dramatically different dynamics observed for the hydrophilic and hydrophobic pores is thus clearly attributable to the pore-water interactions. The contrast between the two pores can be further analyzed by comparing the structures of the interfacial layer, measured through the distributions of water hydrogen and oxygen atom distances, d, relative to the pore wall (Fig. 2(c)). As previously suggested for a set of related nanopores,[18] the key difference originates from the presence of water-silica H-bonds in the hydrophilic case, while water molecules form H-bonds between themselves in the hydrophobic case. This is shown by the distinct peak in the hydrogen distribution around 1.8 Å in the hydrophilic

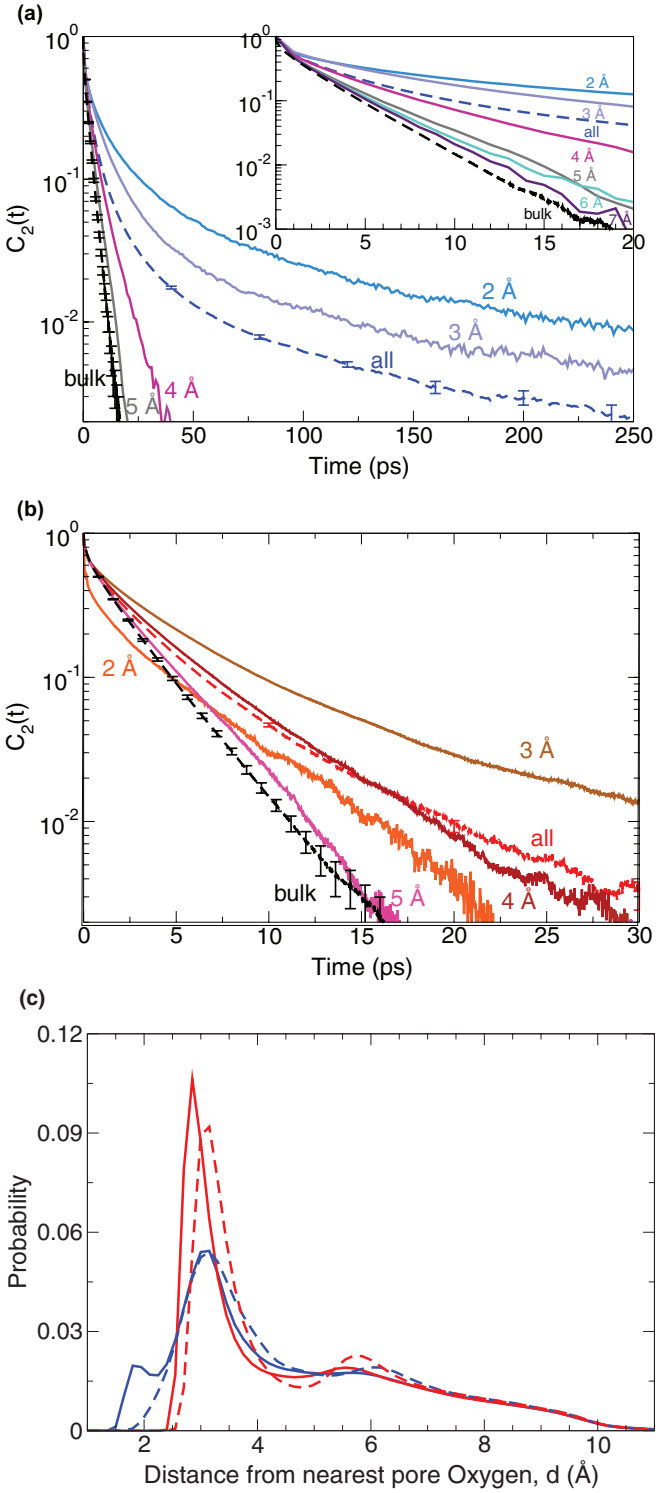

FIG. 2. Reorientational correlation function, $C_2(t; d)$, plotted versus time for water in the hydrophilic (a) and hydrophobic (b) pores for different values of the initial distance d between the hydrogen atom and the pore wall.[45] For comparison, results are shown for bulk water and all confined water molecules. (c) Probability distribution for hydrogen (solid lines) and oxygen (dashed lines) atoms in water as a function of the distance d from the nearest pore oxygen atom. Results are shown for the hydrophilic (blue) and uncharged, hydrophobic (red) pores.

pore, a feature absent in the hydrophobic case. This is also reflected in the oxygen distributions which are displaced further from the surface in the hydrophobic pore, peaking at ~3.1 Å compared to ~2.9 Å in the hydrophilic pore. We will see below how these different structures of the interfacial

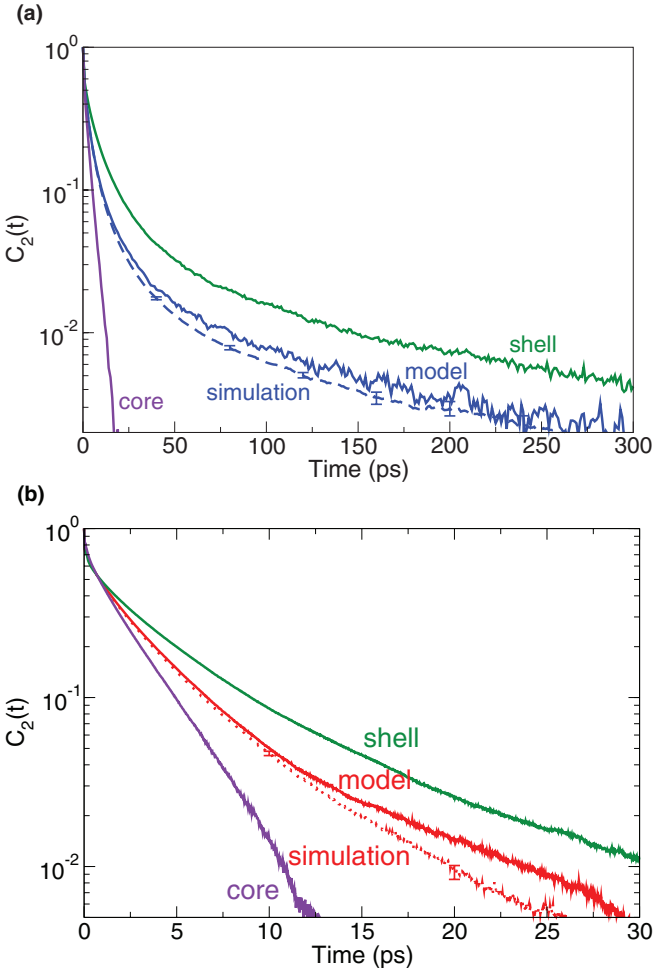

FIG. 3. Comparison between the reorientational correlation functions $C_2(t)$ directly obtained from the simulations (dashes, see Fig. 1) and reconstructed from a two-state model, Eq. (3), (solid lines) combining the displayed core and shell components in the hydrophilic (a) and hydrophobic (b) pores with a shell thickness $\Delta = 3.5$ Å and a pore radius $R = 12$ Å.

water layer cause the dramatic difference in dynamics between the two pores.

Based on this detailed analysis of the $C_2(t; d)$ results, we now examine whether the average decay can be reconstructed within a simplified two-state core/shell model, Eq. (3), with carefully determined decays for the interface and the interior. We approximate the shell contribution $C_2^{\text{shell}}(t)$ as the average of the $C_2(t; d = 2$ Å) and $C_2(t; d = 3$ Å) decays, weighted by the number of water molecules at each distance, while the core contribution is taken to be $C_2(t; d = 7$ Å). Figure 3 shows that such a two-state model provides a very good fit of the global reorientation decay. For the present pore size ($R = 12$ Å), the shell thickness ($\Delta = 3.5$ Å) is not negligible and the $(\Delta/R)^2$ term in Eq. (3) should be included. It is interesting to note that fitting the reorientational decay using Eq. (3) gives $\Delta = 2.8$ Å for both the hydrophilic and hydrophobic pores, a value somewhat smaller than anticipated from the definition of $C_2^{\text{shell}}(t)$.

Our molecular-level study of the water reorientation dynamics therefore shows that the simple assumptions underlying the two-state model, namely the existence of two distinct states, each with homogeneous dynamics, are not

satisfied. The shell contribution is clearly heterogeneous, with a non-exponential relaxation. As shown in Fig. 3, the two-state model can be adapted to provide a satisfactory description of the orientational relaxation if the non-exponential character of the shell contribution is explicitly considered. However, this effective description does not fully address the microscopic origin of the water dynamics. We now address this issue by providing a molecular-level explanation of the non-exponential decay within the interfacial layer and of the dramatically different dynamics within the hydrophilic and hydrophobic interfaces.

V. HYDROGEN-BOND JUMP PICTURE

We analyze the water reorientation dynamics through the recently suggested extended jump model.[24–26] The basic components of this model are that reorientation occurs mainly through large angular jumps associated with changes in the H-bond partner of a given OH moiety, with a minor contribution coming from the "frame" reorientation of the intact H-bond between such jumps.[24,26] This model was shown to describe successfully the water reorientation dynamics next to a broad range of solutes and interfaces,[26] including hydrophobic[47] and hydrophilic interfaces.[48]

Since jumps represent a dominant contribution to the reorientation kinetics (except next to strong H-bond acceptors[49,50]), differences in the reorientation time usually result directly from changes in the jump time, τ_0, which is the inverse rate constant for exchanging H-bonding partners. It can be obtained from the side-side correlation function,

$$C_{AB}(t) = \langle n_A(0)\, n_B(t)\rangle, \tag{4}$$

where $n_A(0) = 1$ when an OH bond is engaged in a H-bond with an initial acceptor, labelled A, and similarly $n_B(t) = 1$ only when the same OH bond has formed a new H-bond by exchanging the acceptor A for a new acceptor B. Thus, the increase in $C_{AB}(t)$ with time measures the time scale for H-bond exchanges and $1 - C_{AB}(t)$ decays exponentially as $\exp(-t/\tau_0)$. Jump times are calculated with absorbing boundary conditions in the product B state and thus correspond to well-defined initial and final states.

In the hydrophilic silica pore, the exposed H-bond acceptor groups are all oxygens but they represent a heterogeneous group since they include bridging oxygens (–Si–O–Si–) as well as silanols (–Si–O–H) and geminals (H–O–Si–O–H), arranged on a rough surface. The decay of the H-bond exchange correlation function, $1 - C_{AB}(t)$, for all water OH groups is thus not single-exponential and a single jump time is not obtainable. It is interesting then to consider the correlation function for each different H-bond acceptor type. This is presented in Fig. 4(a), where $1 - C_{AB}(t)$ is plotted for OH groups initially donating a hydrogen bond to a water oxygen, bridging oxygen, silanol oxygen, and geminal oxygen, respectively. It is clear that these correlation functions also do not exhibit single-exponential dynamics. In other words, a single jump time is not adequate to describe even all OH groups hydrogen bonded to a particular type of H-bond acceptor. However, greater insight into the interfacial water dynamics can be obtained by calculating $C_{AB}(t)$ separately for each initial acceptor on the pore. Specifically, $1 - C_{AB}(t)$ can be calculated for all OH groups H-bonded to a particular, individual silanol oxygen, and the results are shown in Fig. 4(b). This does yield approximately single-exponential decays for

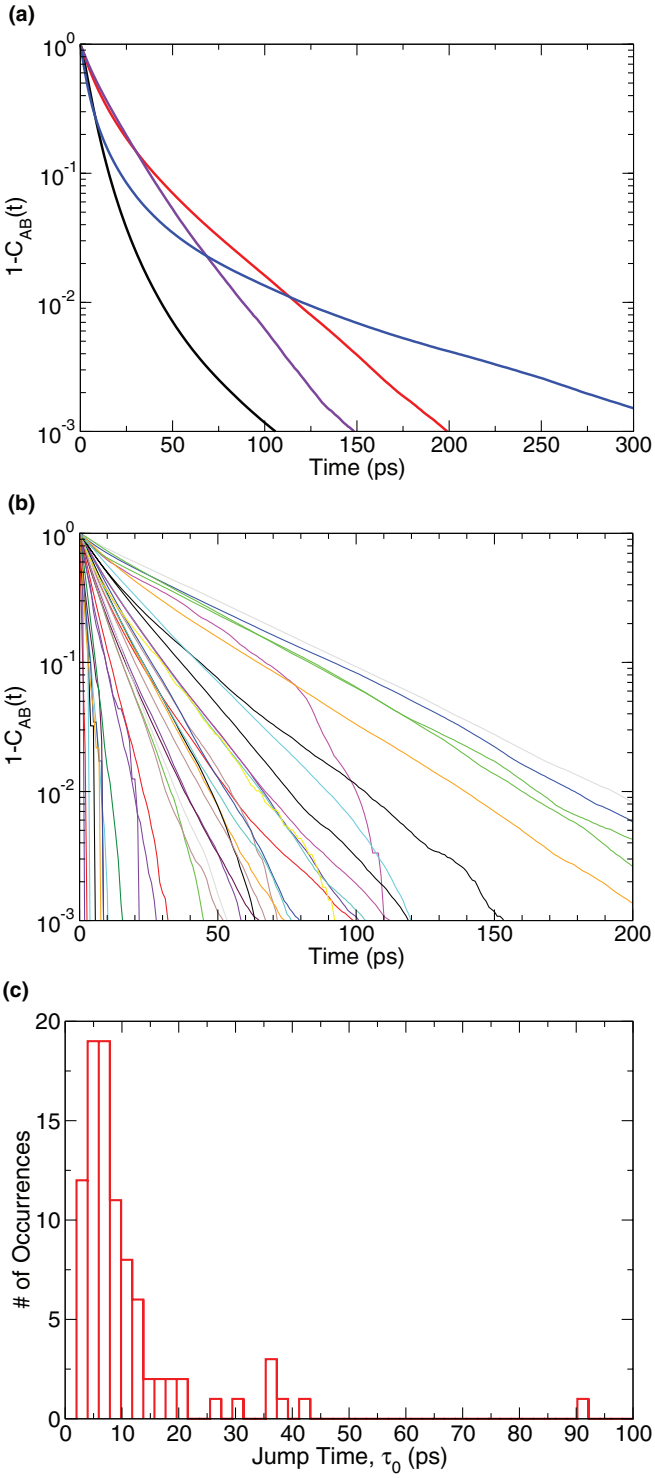

FIG. 4. (a) H-bond exchange correlation function $1 - C_{AB}(t)$, Eq. (4), for OH groups initially H-bonded to water oxygens (black), silanol oxygens (red), geminal oxygens (violet), and bridging oxygens (blue). (b) Same as (a) but each curve corresponds to all OH groups hydrogen bonded to a particular silanol oxygen acceptor. (c) The distribution of single-exponential decay times of $1 - C_{AB}(t)$ for individual acceptors on the pore (silanol, geminal, and bridging oxygens).

each $1 - C_{AB}(t)$. The same analysis has also been carried out for individual geminal and bridging oxygens (not shown), which show similar behavior. The variation in the decay times of the correlation functions in Fig. 4(b) provides a measure of the dynamical heterogeneity within the interfacial layer. It indicates that the origin of the nonexponential decay of the correlation function obtained for all silanol oxygen H-bond acceptors is related to the strong dependence of the jump time on the location of the acceptor on the pore surface. This variation of the jump time, τ_0, with acceptor is also illustrated in Fig. 4(c) where the distribution of τ_0 is plotted; these results are obtained for all individual H-bond accepting oxygens (silanol, geminal, and bridging) based on an automated fitting of the individual acceptor correlation functions, such as those in Fig. 4(b).

Taken together, these results probing the hydrogen-bond exchange times indicate that the waters H-bonded to the surface cannot be viewed, at the molecular-level, as a single population with common dynamics – an observation that is at odds with the implication of a two-state model, since the "shell" state itself includes a broad distribution of sub-states with distinct dynamics. Moreover, it suggests that the nonexponential decay in $C_2(t)$ for OH bonds near the pore surface may arise from this heterogeneity.

As shown previously in other environments, changes in jump times relative to the bulk arise from two factors,[26] the strength of the initial H-bond, if it is not a water-water bond, and the degree of local confinement, that is, excluded volume effects. In the hydrophilic pore, the different hydrogen-bond acceptors (bridging oxygens, silanols, and geminals) combined with the roughness of the pore wall lead to a broad distribution of jump times.[51] In the hydrophobic pore, water molecules cannot form H-bonds with the interface and most water OH groups lie approximately tangent to the pore wall.[47] For these OHs, reorientation dynamics is governed only by the local excluded volume, e.g., by the surface roughness. This explains why the spread in the reorientation time distribution is reduced in the hydrophobic case, leading to a quasi single-exponential behavior as seen in Figs. 1(b) and 2(b). Indeed, recent work on model flat silica surfaces suggests that interfacial water dynamics could be accelerated by reducing the surface polarity.[48]

VI. CONCLUDING REMARKS

Water reorientation dynamics in a nanoscale, hydrophilic silica pore and compared with water confined in a hydrophobic silica pore and the bulk liquid. The reorientation of the OH-bond is dramatically affected by confinement within the ~2.4 nm hydrophilic pore. The longest time scale for reorientation, measured by the $C_2(t)$ reorientational correlation function, is ~2.6 ps in the bulk liquid. This is lengthened by roughly two orders-of-magnitude for water in the hydrophilic pores and is best fit by a power-law decay. The results are sensitive to the pore interactions. A hydrophobic pore, obtained by setting the surface charges to zero, gives dynamics that differ from the bulk primarily by the appearance of an additional timescale that is ~2.5 times longer than that of bulk water.

A two-state, or core-shell, model is a reasonable, but incomplete, molecular-level description of confined water in the hydrophilic silica pores. Specifically, the total $C_2(t)$ reorientational correlation function is well described by a sum of the correlation functions for water molecules at the pore surface (in the shell) and waters in the interior (core), as predicted by the model. However, in contrast with the assumptions of the two-state model, the dynamics within each state is not homogeneous. The power-law decay of $C_2(t)$ in the hydrophilic pore appears to be a consequence of the heterogeneity of the surface – the shell waters themselves exhibit a power-law decay – and indicates the difficulties with identifying water at the pore interface as a single population. On the other hand, the dynamics can be meaningfully interpreted by examining the reorientation in terms of a hydrogen-bond jump model. The dynamics associated with the exchange of hydrogen-bonding partners for a given hydrogen-bond acceptor on the pore surface (silica or silanol oxygen) is nearly single exponential.

ACKNOWLEDGMENTS

W.H.T. acknowledges support for this work from the Chemical Sciences, Geosciences, and Biosciences Division, Office of Basic Energy Sciences, Office of Science, U.S. Department of Energy (DOE).

[1] S. Bernèche and B. Roux, Nature London **414**, 73 (2001).
[2] M. D. Fayer and N. E. Levinger, Annu. Rev. Anal. Chem. **3**, 89 (2010).
[3] N. E. Levinger and L. A. Swafford, Annu. Rev. Phys. Chem. **60**, 385 (2009).
[4] D. E. Moilanen, I. R. Piletic, and M. D. Fayer, J. Phys. Chem. C **111**, 8884 (2007).
[5] K. Gethard, O. Sae-Khow, and S. Mitra, ACS Appl. Mater. Interfaces **3**, 110 (2011).
[6] P. Gallo, M. Rovere, and S.-H. Chen, J. Phys. Chem. Lett. **1**, 729 (2010).
[7] W. H. Thompson, Annu. Rev. Phys. Chem. **62**, 599 (2011).
[8] A. Scodinu and J. T. Fourkas, J. Phys. Chem. B **106**, 10292 (2002).
[9] R. A. Farrer and J. T. Fourkas, Acc. Chem. Res. **36**, 605 (2003).
[10] N. Giovambattista, P. J. Rossky, and P. G. Debenedetti, Phys. Rev. E **73**, 041604 (2006).
[11] N. Giovambattista, P. J. Rossky, and P. G. Debenedetti, J. Phys. Chem. B **113**, 13723 (2009).
[12] C. A. Cerdeiriña, P. G. Debenedetti, P. J. Rossky, and N. Giovambattista, J. Phys. Chem. Lett. **2**, 1000 (2011).
[13] R. Mancinelli, F. Bruni, and M. A. Ricci, J. Phys. Chem. Lett. **1**, 1277 (2010).
[14] M.-C. Bellissent-Funel, J. Lal, and L. Bosio, J. Chem. Phys. **98**, 4246 (1993).
[15] S. Stapf and R. Kimmich, J. Chem. Phys. **103**, 2247 (1995).
[16] T. Takamuku, M. Yamagami, H. Wakita, Y. Masuda, and T. Yamaguchi, J. Phys. Chem. B **101**, 5730 (1997).
[17] H. Thompson, A. K. Soper, M. A. Ricci, F. Bruni, and N. T. Skipper, J. Phys. Chem. B **111**, 5610 (2007).
[18] J. Jelassi, T. Grosz, I. Bako, M. C. Bellissent-Funel, J. C. Dore, H. L. Castricum, and R. Sridi-Dorbez, J. Chem. Phys. **134**, 064509 (2011).
[19] L. Frunza, A. Schönhals, H. Kosslick, and S. Frunza, Eur. Phys. J. E **26**, 379 (2008).
[20] P. Gallo, M. Rovere, and S.-H. Chen, J. Phys.: Condens. Matter **22**, 284102 (2010).
[21] A. A. Milischuk and B. M. Ladanyi, J. Chem. Phys. **135**, 174709 (2011).
[22] G. Liu, Y.-Z. Li, and J. Jonas, J. Chem. Phys. **95**, 6892 (1991).
[23] J. P. Korb, A. Delville, S. Xu, G. Demeulenaere, P. Costa, and J. Jonas, J. Chem. Phys. **101**, 7074 (1994).
[24] D. Laage and J. T. Hynes, Science **311**, 832 (2006).
[25] D. Laage and J. T. Hynes, J. Phys. Chem. B **112**, 14230 (2008).

[26]D. Laage, G. Stirnemann, F. Sterpone, R. Rey, and J. T. Hynes, Annu. Rev. Phys. Chem. **62**, 395 (2011).
[27]The DL_POLY molecular simulation package. See http://www.ccp5.ac.uk/DL_POLY.
[28]The TOWHEE Monte Carlo molecular simulation program. See http://towhee.sourceforge.net.
[29]H. J. C. Berendsen, J. R. Grigera, and T. P. Straatsma, J. Phys. Chem. **91**, 6269 (1987).
[30]T. S. Gulmen and W. H. Thompson, Langmuir **22**, 10919 (2006).
[31]S. Nosé, Mol. Phys. **52**, 255 (1984).
[32]W. G. Hoover, Phys. Rev. A **31**, 1695 (1985).
[33]D. P. Shoemaker, C. W. Garland, and J. W. Nibler, *Experiments in Physical Chemistry*, (McGraw-Hill, New York, 1989).
[34]Y. S. Lin, P. A. Pieniazek, M. Yang, and J. L. Skinner, J. Chem. Phys. **132**, 174505 (2010).
[35]S. R. V. Castrillón, N. Giovambattista, I. A. Aksay, and P. G. Debenedetti, J. Phys. Chem. B **113**, 1438 (2009).
[36]H. J. Bakker, Y. L. A. Rezus, and R. L. A. Timmer, J. Phys. Chem. A **112**, 11523 (2008).
[37]C. Mattea, J. Qvist, and B. Halle, Biophys. J. **95**, 2951 (2008).
[38]D. Andreatta, J. L. P. Lustres, S. A. Kovalenko, N. P. Ernsting, C. J. Murphy, R. S. Coleman, and M. A. Berg, J. Am. Chem. Soc. **127**, 7270 (2005).
[39]S. Sen, D. Andreatta, S. Y. Ponomarev, D. L. Beveridge, and M. A. Berg, J. Am. Chem. Soc. **131**, 1724 (2009).
[40]K. E. Furse and S. A. Corcelli, J. Am. Chem. Soc. **133**, 720 (2011).
[41]P. A. Pieniazek, Y.-S. Lin, J. Chowdhary, B. M. Ladanyi, and J. L. Skinner, J. Phys. Chem. B **113**, 15017 (2009).
[42]D. E. Moilanen, E. E. Fenn, D. B. Wong, and M. D. Fayer, J. Chem. Phys. **131**, 014704 (2009).
[43]I. R. Piletic, D. E. Moilanen, D. B. Spry, N. E. Levinger, and M. D. Fayer, J. Phys. Chem. A **110**, 4985 (2006).
[44]C. M. Morales and W. H. Thompson, J. Phys. Chem. A **113**, 1922 (2009).
[45]For a given nominal distance, d, the correlation function $C_2(t; d)$ is obtained by averaging over all hydrogen atom distances within 0.5 Å of d. For example, $C_2(t; d = 2\,\text{Å})$ is obtained by averaging over all OH bonds with $H\cdots O_{pore}$ distances at $t = 0$ within the range 1.5–2.5 Å.
[46]We note that the transient nature of non-hydrogen-bonded OH groups near the hydrophobic pore interface is virtually unchanged from that of bulk water. That is, the distribution of waiting times for OH groups which are not hydrogen bonded to form a hydrogen bond is virtually the same for water in the hydrophobic pore (decaying to zero in less than 1 ps) as in bulk water.
[47]G. Stirnemann, P. J. Rossky, J. T. Hynes, and D. Laage, Faraday Discuss. **146**, 263 (2010).
[48]G. Stirnemann, S. R. V. Castrillon, J. T. Hynes, P. J. Rossky, P. G. Debenedetti, and D. Laage, Phys. Chem. Chem. Phys. **13**, 19911 (2011).
[49]F. Sterpone, G. Stirnemann, J. T. Hynes, and D. Laage, J. Phys. Chem. B **114**, 2083 (2010).
[50]J. Boisson, G. Stirnemann, D. Laage, and J. T. Hynes, Phys. Chem. Chem. Phys. **13**, 19895 (2011).
[51]The present simulations are based on the classical SPC/E water force field. Next to strong H-bond acceptor sites, an explicit description of polarizability and three-body effects may be needed.